

# Discrete Analysis of Stiffened Composite Cylindrical Shells

James Ting-Shun Wang\*

Georgia Institute of Technology, Atlanta, Georgia

and

Teh-Min Hsu†

Chevron Oil Field Research Company, La Habra, California

Composite circular cylindrical shells with closed ends stiffened by equally spaced stringers and rings subjected to combinations of uniform internal pressure, constant temperature change, and axial load are investigated. A representative region consisting of a stringer, a ring, and the skin bounded between sections midway between adjacent rings and stringers are considered in the analysis. The stringer, ring, and skin are treated as separate components. Equations governing these individual components are coupled through interacting normal and shear loads. The present analysis, which accounts for the interacting shear forces between the skin and stiffeners, and allows for direct accounting of closed-end effects, contains improvements over an earlier analysis. Some numerical results are presented.

## Nomenclature

$a$	= shell radius
$b$	= stringer spacing
$e_r, e_s$	= eccentricities
$(EA)_r, (EA)_s$	= extensional stiffnesses
$(EI)_r, (EI)_s$	= flexural stiffnesses
$h$	= skin thickness
$L$	= ring spacing
$M_r, M_s$	= bending moments
$M_x, M_y, M_{xy}$	= stress couples
$N_x, N_y, N_{xy}$	= stress resultants
$P_r, P_s$	= axial forces
$p$	= normal loading component on skin
$p_r, p_s$	= normal loading components
$q_x, q_y$	= tangential loading components on skin
$q_r, q_s$	= tangential loading components
$Q_x, Q_y$	= transverse shear stress resultants
$R_0$	= ring radius
$T$	= temperature change
$u, v, w$	= midplane displacements of skin
$v_r, w_r, v_s, w_s$	= displacements of ring and stringer
$x, y, z$	= surface coordinates
$\sigma_x, \sigma_y, \tau_{xy}$	= stress components
$\epsilon_x, \epsilon_y, \gamma_{xy}$	= strain components
$\phi$	= Airy stress function
<b>Subscripts</b>	
$r$	= ring
$s$	= stringer

## Introduction

ORTHOGONALLY stiffened cylindrical shells have been widely used in aircraft fuselage designs and many other structural applications. For vibration and buckling analyses, it may be satisfactory to smear the stiffness of the stiffeners and treat the stiffened shell as an equivalent orthotropic shell. Numerous papers are cited in Ref. 1. Such smeared analyses give reasonable results for shells having closely spaced stiffeners, where each half wave in the cir-

cumferential direction contains a number of stiffeners. However, for the buckling and vibration of sparsely stiffened shells or for the stress analysis of stiffened shells, it is desirable to treat the stiffeners and skin as separate structural components so that the local mode of vibration or buckling and local peak stresses and strains may be determined. Such discrete analysis for vibration and buckling have been considered by many authors, e.g., Refs. 2-7. A stress analysis is presented in Ref. 1 for isotropic materials. Following the general concept of analysis presented in Ref. 1, cylindrical shells made of composite materials are considered in the present study. The closed-end effect is directly incorporated in the general analysis instead of the rather cumbersome separate investigation in Ref. 1. While the effect of interacting shear forces between the skin and stiffeners is not accounted for therein, it is included in the present analysis. In addition, the effect of temperature change is also considered in this study. Some numerical results are presented for illustrative purposes.

## General Analysis

Orthotropic circular cylindrical shells stiffened by equally spaced stringers and rings subjected to internal pressure and temperature change are investigated. The linear elastic theory is used in the study. The skin and stiffeners are treated as separate components coupled through unknown interacting normal and shear loads. These interacting loads are determined when the continuity conditions in the displacements are applied. A representative region with the boundary along the midlines between adjacent rings and stringers as shown in Fig. 1 will be considered for the analysis. The governing equations for the stiffeners and skin and their general solutions expressed in terms of interacting loads will be presented first. These unknown interacting loads will be determined when the continuities of the displacements for the skin and stiffeners are satisfied.

### Stringer

Referring to Fig. 2, the equilibrium condition leads to

$$\frac{d}{dx}(P_s, V_s, M_s) = (p^s, -q^s, -V_s - p^s e_s) \quad (1)$$

in which  $P_s$ ,  $V_s$ , and  $M_s$  are the axial force, shear force, and bending moment, respectively;  $p^s$  and  $q^s$  the interacting

Received Feb. 6, 1984; revision submitted Nov. 21, 1984. Copyright © American Institute of Aeronautics and Astronautics, Inc., 1985. All rights reserved.

\*Professor, School of Engineering Science and Mechanics.

†Senior Research Engineer. Member AIAA.

loads;  $e_s$  the eccentricity; and  $w_s$  the transverse displacement. The relationship between internal loads and displacements are

$$(EA)_s \frac{du_s}{dx} = P_s + P_{st} \quad (2)$$

$$(EI)_s \frac{d^2 w_s}{dx^2} = M_s + M_{st} \quad (3)$$

in which

$$P_{st} = \{E_s \alpha_s T dA \quad (4)$$

$$M_{st} = \{E_s z_s \alpha_s T dA \quad (5)$$

The temperature change  $T$ , coefficient  $E_s$ , and thermal coefficient  $\alpha_s$  are considered to be independent of  $x$ . As a result,  $P_{st}$  and  $M_{st}$  are constants in the analysis. Substituting Eqs. (2) and (3) into Eq. (1) and combining, one subsequently obtains the following governing differential equations:

$$(EA)_s \frac{d^2 u_s}{dx^2} = p^s \quad (6)$$

$$(EI)_s \frac{d^4 w_s}{dx^4} = q^s - e_s \frac{dp^s}{dx} \quad (7)$$

where  $(EA)_s$  and  $(EI)_s$  are the effective extensional and flexural rigidities, respectively. Representing the following quantities by appropriate Fourier series:

$$(w_s, e_s, q^s) = (W_{s0}, \epsilon_{s0}, 0) + \sum_m (W_{sm}, \epsilon_{sm}, q_m^s) \cos \alpha_m x \quad (8)$$

$$p^s = \sum_m p_m^s \sin \alpha_m x \quad (9)$$

and substituting them subsequently into Eqs. (6) and (7), one obtains

$$W_{sm} = A_m^s q_m^s + B_m^s p_m^s \quad (10)$$

$$\epsilon_{sm} = G_m^s p_m^s \quad (11)$$

in which  $\alpha_m = m\pi/L$ ,  $L$  is the ring spacing, and  $m$  takes on even integers.

$$A_m^s = \frac{1}{(EI)_s \alpha_m^4 + \bar{P}_s \alpha_m^2} \quad (12)$$

$$B_m^s = -e_s \alpha_m A_m^s \quad (13)$$

$$G_m^s = -\frac{1}{(EI)_s \alpha_m} \quad (14)$$

#### Ring

Referring to Fig. 3, the equilibrium equations are

$$\frac{dP_r}{ds} + \frac{V_r}{R_0} = p^r \left(1 + \frac{e_r}{R_0}\right) \quad (15)$$

$$\frac{dV_r}{ds} - \frac{P_r}{R_0} = -q^r \left(1 + \frac{e_r}{R_0}\right) \quad (16)$$

$$\frac{dM_r}{ds} + V_r + p^r \left(1 + \frac{e_r}{R_0}\right) e_r = 0 \quad (17)$$

in which  $s$ , measured from the midpoint between stringers, is the coordinate along the neutral plane of the ring;  $P_r$ ,  $V_r$ ,

and  $M_r$  are the axial force, shear force, and bending moment, respectively;  $p^r$  and  $q^r$  are interacting loads;  $e_r$  is the eccentricity;  $w_r$  is the transverse displacement; and  $R_0$  is the radius of the ring. The relations between internal loads and displacements are

$$(EA)_r e_r = (EA)_r \left( \frac{dv_r}{ds} + \frac{w_r}{R_0} \right) = (P_r + P_{rt}) \quad (18)$$

$$(EI)_r \left( -\frac{dv_r}{R_0 ds} + \frac{d^2 w_r}{ds^2} \right) = (M_r + M_{rt}) \quad (19)$$

in which

$$P_{rt} = \{E_r \alpha_r T dA \quad (20)$$

$$M_{rt} = \{z_r E_r \alpha_r T dA \quad (21)$$

are considered to be independent of  $y$ ,  $v_r$  is the tangential displacement of the ring, and  $(EA)_r$  and  $(EI)_r$  are the effective extensional and flexural stiffness, respectively.

Substituting Eq. (19) into Eq. (17), one obtains

$$V_r = (EI)_r \left( \frac{d^2 v_r}{R_0 ds^2} - \frac{d^3 w_r}{ds^3} \right) - p^r e_r \left( 1 + \frac{e_r}{R_0} \right) + \frac{dM_{rt}}{ds} \quad (22)$$

Equations (15) and (16) may be expressed in terms of displacements when equations (18) and (19) are used. They are

$$\frac{d^2 v_r}{ds^2} = a_{r1} \frac{d^3 w_r}{ds^3} + a_{r2} \frac{dw_r}{ds} + a_{r3} p^r + S_r \frac{dT_r}{ds} \quad (23)$$

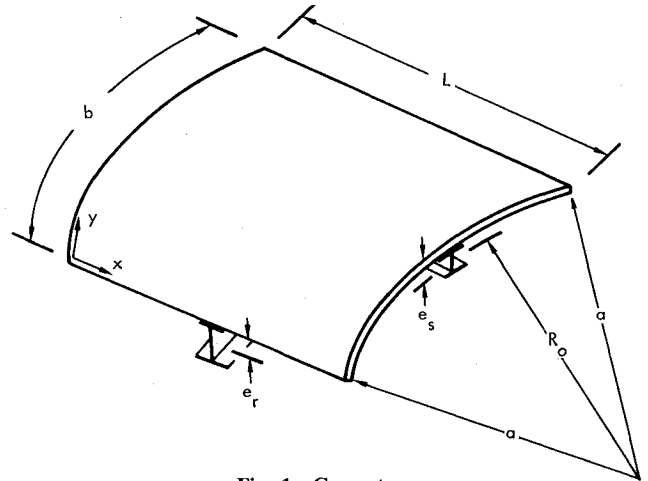


Fig. 1 Geometry.

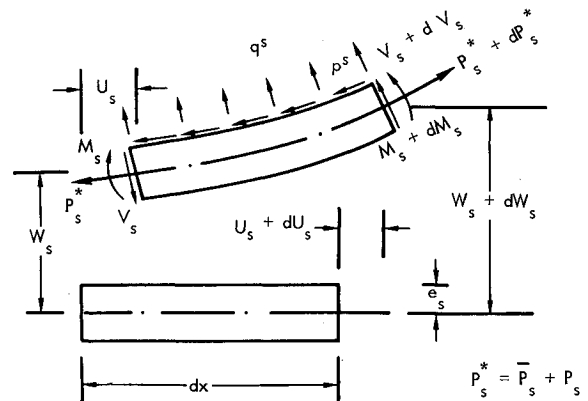


Fig. 2 Stringer.

$$\frac{1}{R_0} \left[ (EI)_r \frac{d^3 v_r}{ds^3} - (EA)_r \frac{dv_r}{ds} \right] - \left[ (EI)_r \frac{d^4 w_r}{ds^4} + (EA)_r \frac{w_r}{R_0^2} \right] + \bar{P}_r \frac{d^2 w_r}{ds^2} = \left( 1 + \frac{e_r}{R_0} \right) \left( e_r \frac{dp_r}{ds} - q_r \right) - \frac{P_{rt}}{R_0} - \frac{d^2 M_{rt}}{ds^2} \quad (24)$$

where

$$a_{r1} = S_r \frac{(EI)_r}{R_0}, \quad a_{r2} = -S_r \frac{(EA)_r}{R_0}, \quad a_{r3} = S_r \left( 1 + \frac{e_r}{R_0} \right)^2$$

$$S_r = \frac{R_0^2}{R_0^2 (EA)_r + (EI)_r}, \quad T_r = P_{rt} - \frac{M_{rt}}{R_0}$$

Inasmuch as the skin thickness is small,  $(R_0 + e_r) = a$  will be used in the subsequent derivations. Equations (23) and (24) may be combined into the following equation:

$$\beta_1^* \frac{d^5 w_r}{ds^5} + \beta_2^* \frac{d^3 w_r}{ds^3} + \beta_3^* \frac{dw_r}{ds} = \frac{a_{r3}}{R_0} \left[ (EA)_r p_r - (EI)_r \frac{d^2 p_r}{ds^2} \right] + e_r \frac{a}{R_0} \frac{d^2 p_r}{ds^2} - \frac{a}{R_0} \frac{dq_r}{ds} + \frac{S_r}{R_0} \left[ (EA)_r \frac{dT_r}{ds} - (EI)_r \frac{d^3 T_r}{ds^3} \right] + \frac{d^3 M_{rt}}{ds^3} - \frac{1}{R_0} \frac{dP_{rt}}{ds} \quad (25)$$

where

$$\beta_1^* = \frac{1}{R_0} (EI)_r (a_{r1} - R_0), \quad \beta_2^* = -\frac{1}{R_0} [(EI)_r a_{r2} - (EA)_r a_{r1}]$$

$$\beta_3^* = \frac{(EA)_r (EI)_r}{R_0^2 [R_0^2 (EA)_r + (EI)_r]}$$

The transverse displacement, strain, and interacting loads are represented by the appropriate Fourier series as follows:

$$(W_r, \epsilon_r, q_r) = (W_{r0}, \epsilon_{r0}, \frac{1}{2} q_0^r) + \sum_n (W_{rn}, \epsilon_{rn}, q_n^r) \cos \beta_n y \quad (26)$$

$$p_r = \sum_n p_n^r \sin \beta_n y \quad (27)$$

in which  $\beta_n = n\pi/b$ . The variable  $y$  is the circumferential coordinate along the mid-surface of the skin. Hence,

$$y = (as/R_0) \quad (28)$$

The extensional strain displacement relation is

$$\epsilon_r = \frac{\partial v_r}{\partial s} + \frac{w_r}{R_0} \quad (29)$$

Using Eqs. (24) and (25) and integrating subsequently along  $y$  from 0 to  $b$ , one finds

$$\epsilon_{r0} = W_{r0}/R_0 \quad (30)$$

Substituting Eq. (26) into Eq. (25), one obtains

$$W_{rn} = C_n^r q_n^r + D_n^r p_n^r \quad (31)$$

where  $C_n^r$  and  $D_n^r$  are known constants.

Differentiating Eq. (29) with respect to  $s$  and subsequently using Eqs. (23) and (31), one obtains

$$\epsilon_{rn} = A_n^r q_n^r + B_n^r p_n^r \quad (32)$$

where  $A_n^r$  and  $B_n^r$  are known constants.

Since  $V_r = 0$  at  $y = 0$  and  $b$ ,  $V_r$  may be represented by the following series:

$$V_r = \sum_n V_{rn} \sin \beta_n y \quad (33)$$

As a result,  $\epsilon_{r0}$  may be determined from Eq. (16) in conjunction with Eqs. (18) and (26-28) as follows:

$$\epsilon_{r0} = \frac{a}{2(EA)_r} q_0^r + \frac{1}{(EA)_r} P_{rt} \quad (34)$$

Consequently, one obtains from Eq. (30)

$$W_{r0} = \frac{R_0 a}{2(EA)_r} q_0^r + \frac{R_0}{(EA)_r} P_{rt} \quad (35)$$

#### Shell

The sign convention and some symbols are shown in Fig. 4. The equilibrium equations based on Donnell's approximations are

$$N_{x,x} + N_{yx,y} + q_x = 0 \quad (36)$$

$$N_{xy,x} + N_{y,y} + q_y = 0 \quad (37)$$

$$Q_{x,x} + Q_{y,y} - (N_y/a) - q = 0 \quad (38)$$

$$M_{x,x} + M_{yx,y} - Q_x = 0 \quad (39)$$

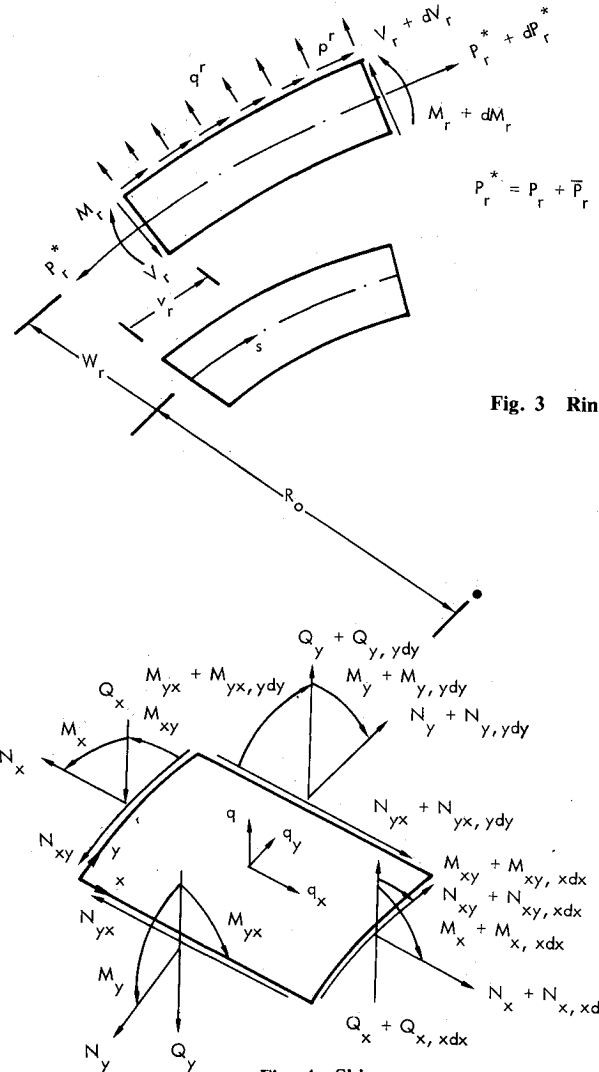


Fig. 3 Ring.

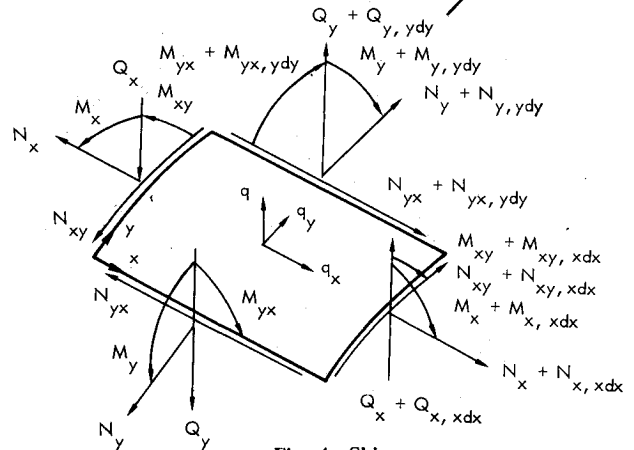


Fig. 4 Skin.

$$M_{xy,x} + M_{y,y} - Q_y = 0 \quad (40)$$

where  $a$  is the radius of the cylinder;  $N_x$ ,  $N_y$ ,  $N_{xy}$ ,  $Q_x$ , and  $Q_y$  stress resultants;  $M_x$ ,  $M_y$ , and  $M_{xy}$  stress couples;  $q_x$ ,  $q_y$ , and  $q$  surface loading components in the  $x$ ,  $y$  and normal directions, respectively. The strain displacement relations are

$$\epsilon_x = \epsilon_x^0 - z w_{,xx} \quad (41)$$

$$\epsilon_y = \epsilon_y^0 - z w_{,yy} \quad (42)$$

$$\gamma_{xy} = \gamma_{xy}^0 - 2z w_{,xy} \quad (43)$$

where  $z$  is the normal coordinate,  $\epsilon_x^0$ ,  $\epsilon_y^0$ , and  $\gamma_{xy}^0$  are strain components at  $z=0$ , which relate to displacements at  $z=0$  as follows:

$$\epsilon_x^0 = u_{,x} \quad (44)$$

$$\epsilon_y^0 = v_{,y} + w/a \quad (45)$$

$$\gamma_{xy}^0 = u_{,y} + v_{,x} \quad (46)$$

The stress-strain relations for orthotropic materials accounting for the thermal effect are

$$\{N\} = [A] \{\epsilon^0\} - \{N_t\} \quad (47)$$

$$\{\epsilon^0\} = [A]^{-1} \{N\} + \{N_t^*\} \quad (48)$$

$$\{M\} = [D] \{\kappa\} - \{M_t\} \quad (49)$$

$$\{N_t\} = \int_{-h/2}^{h/2} [C] \{\alpha\} T dz \quad (50)$$

$$\{N_t^*\} = [A]^{-1} \{N_t\} \quad (51)$$

$$\{M_t\} = \int_{-h/2}^{h/2} z [C] \{\alpha\} T dz \quad (52)$$

where  $\kappa$  and  $\alpha$  are the curvature changes and thermal expansion coefficients, respectively.

The temperature change is considered to be independent of  $x$  and  $y$ . Consequently,  $N_{xt}$ ,  $N_{yt}$ ,  $M_{xt}$ , and  $M_{yt}$  are constants. For a given layup, the material constants involved in Eqs. (47-49) can be determined from classical laminate theory. The relevant compatibility equation is

$$\epsilon_{x,yy}^0 + \epsilon_{y,xx}^0 - \gamma_{xy,xy}^0 = - (1/a) w_{,xx} \quad (53)$$

Introducing the Airy stress function  $\phi$  such that

$$N_x = \phi_{,yy} - \int q_x dx \quad (54)$$

$$N_y = \phi_{,xx} - \int q_y dy \quad (55)$$

$$N_{xy} = -\phi_{,xy} \quad (56)$$

which satisfy Eqs. (36) and (37), and using Eq. (48) in conjunction with Eqs. (54), (55), and (56), the compatibility equation (53) becomes

$$B_{22} \phi_{,xxxx} + (2B_{12} + B_{66}) \phi_{,xxyy} + B_{11} \phi_{,yyyy} = (B_{21} \int q_x dx + B_{22} \int q_y dy)_{,xx} + (B_{11} \int q_x dx + B_{12} \int q_y dy)_{,yy} - (1/a) w_{,xx} \quad (57)$$

Combining Eqs. (38-40) in conjunction with Eqs. (49) and (55), one obtains

$$D_{11} w_{,xxxx} + 2(D_{12} + 2D_{66}) w_{,xxyy} + D_{22} w_{,yyyy} = -q - (1/a) \phi_{,xx} + (1/a) \int q_y dy \quad (58)$$

The loading functions on the shell are

$$q_x = p^s f(y) \quad (59)$$

$$q_y = p^r g(x) \quad (60)$$

$$q = q^s f^*(y) + q^r g^*(x) - p \quad (61)$$

The functions  $f(y)$ ,  $g(x)$ ,  $f^*(y)$ , and  $g^*(x)$  describe the variations of interacting loads across the width of the stiffeners. Since the deformation of the stiffener cross sections is not considered in this analysis, these functions must be reasonably assumed. A few distributions for  $f(y)$  or  $f^*(y)$ , for  $y$  ranging from  $(b/2 - c_s/2)$  to  $(b/2 + c_s/2)$ , are listed in Table 1.

The quantity  $c_s$  is the flange width of the stringer. The same forms of distribution are applicable for  $g(x)$  and  $g^*(x)$  by simply changing  $y$ ,  $b$ , and  $c_s$  in Table 1 by  $x$ ,  $L$ , and  $c_r$ , respectively, with  $c_r$  being the flange width of the ring.

Expanding the surface loading functions given in Eqs. (59-61) into appropriate Fourier series results in

$$q_x = \sum_m \sum_n q_{xmn} \sin \alpha_m x \cos \beta_n y \quad (62)$$

$$q_y = \sum_n \sum_m q_{ymn} \cos \alpha_m x \sin \beta_n y \quad (63)$$

$$q = \sum_m \sum_n q_{mn} \cos \alpha_m x \cos \beta_n y \quad (64)$$

where  $m$  and  $n$  take on even integers because of symmetry. Through Eqs. (59-61), the Fourier coefficients in Eqs. (62-64) are related to  $p_m^s$ ,  $q_m^s$ ,  $p_n^r$ , and  $q_n^r$  shown in Eqs. (8), (9), (26), and (27), respectively, as follows:

$$(q_{xm0}, q_{xmn}) = \left( \frac{1}{b} f_n \right) p_m^s \quad (65)$$

$$(q_{y0n}, q_{ymn}) = \left( \frac{1}{L} g_m \right) p_n^r \quad (66)$$

$$(q_{00}, q_{0n}, q_{m0}) = \left( \frac{1}{2L} q_0^r - p, \frac{1}{L} q_n^r, \frac{1}{b} q_m^s + \frac{1}{2} g_m^* q_0^r \right) \quad (67)$$

$$q_{mn} = f_n^* q_m^s + g_m^* q_n^r \quad (68)$$

in which

$$(f_n, f_n^*) = \frac{2}{b} \int_0^b (f, f^*) \cos \beta_n y dy \quad (69)$$

Table 1 Distribution of  $f(y)$  or  $f^*(y)$

Type of distribution	$f(y)$ or $f^*(y)$
Concentrated	$\delta[y - (b/2)]$
Uniform	$1/c_s$
Linear	$\frac{2}{c_s} \left[ \left( 1 - \frac{b}{c_s} \right) + 2 \frac{y}{c_s} \right]$ for $\frac{b}{2} - \frac{c_s}{2} < y < 0$
	$\frac{2}{c_s} \left[ \left( 1 + \frac{b}{c_s} \right) - 2 \frac{y}{c_s} \right]$ for $0 < y < \frac{b}{2} + \frac{c_s}{2}$
Cosine	$\frac{\pi}{2c_s} \cos \frac{\pi}{c_s} \left( y - \frac{b}{2} \right)$

$$(g_m, g_m^*) = \frac{2}{L} \int_0^L (g, g^*) \cos \alpha_m x dx \quad (70)$$

The general solutions for transverse displacement, extensional strains, and Airy stress function are represented in the following general form:

$$w = \sum_m \sum_n W_{mn} \cos \alpha_m x \cos \beta_n y \quad (71)$$

$$\begin{Bmatrix} \epsilon_x \\ \epsilon_y \end{Bmatrix} = \sum_m \sum_n \begin{Bmatrix} X_{mn} \\ Y_{mn} \end{Bmatrix} \cos \alpha_m x \cos \beta_n y + \begin{Bmatrix} N_{xt}^* \\ N_{yt}^* \end{Bmatrix} \quad (72)$$

$$\begin{aligned} \phi = \sum_m \sum_n \phi_{mn} \cos \alpha_m x \cos \beta_n y + \frac{1}{2} (A_{11} X_{00} + A_{12} Y_{00} - N_{x1}) y^2 \\ + \frac{1}{2} (A_{21} X_{00} + A_{22} Y_{00} - N_{y1}) x^2 \end{aligned} \quad (73)$$

Clearly, the value of  $\phi_{00}$  is immaterial and is taken to be zero.

Substituting Eqs. (62-73) into Eqs. (57) and (58), one obtains the following relations by comparing like terms:

$$(1/2L) q_0' - p + (1/a) (A_{21} X_{00} + A_{22} Y_{00} - N_{y1}) = 0 \quad (74)$$

$$\rho_{mn} W_{mn} - (1/a) \alpha_m^2 \phi_{mn} = -f_n^* q_m^s - g_m^* q_n' - (1/\beta_n a) g_m p_n' \quad (75)$$

$$-(1/a) \alpha_m^2 W_{mn} + \beta_m \phi_{mn} = b_{mn} p_m^s + d_{mn} p_n' \quad (76)$$

in which all coefficients are known constants.

Solving Eqs. (75) and (76) simultaneously, one obtains

$$W_{mn} = \bar{A}_{mn} q_m^s + \bar{B}_{mn} p_m^s + \bar{C}_{mn} q_n' + \bar{D}_{mn} p_n' \quad (77)$$

$$\phi_{mn} = E_{mn} q_m^s + F_{mn} p_m^s + G_{mn} q_n' + H_{mn} p_n' \quad (78)$$

except for  $W_{00}$ . The coefficient in Eqs. (77) and (78) can be explicitly expressed in terms of known quantities.

Substituting Eqs. (54-56) in conjunction with Eqs. (62-73) and (78) into Eq. (48), one obtains

$$X_{mn} = A_{mn}^u q_m^s + B_{mn}^u p_m^s + C_{mn}^u q_n' + D_{mn}^u p_n' \quad (79)$$

$$Y_{mn} = A_{mn}^v q_m^s + B_{mn}^v p_m^s + C_{mn}^v q_n' + D_{mn}^v p_n' \quad (80)$$

#### Continuity Conditions and Solutions

So far, the general solutions for strains and transverse displacements for stringers, rings, and the skin except  $\epsilon_{s0}$ ,  $W_{r0}$ ,  $X_{00}$ ,  $Y_{00}$ , and  $W_{00}$  are expressed in terms of the interacting loads. Expressions for  $\epsilon_{s0}$ ,  $W_{r0}$ ,  $X_{00}$ ,  $Y_{00}$ , and  $W_{00}$  will be established later. Note that

$$Y_{00} = W_{00}/a \quad (81)$$

In order to maintain continuous deformation of the stiffeners and skin along the attachment lines, the following relations must be satisfied:

1) Along  $x = L/2$ ,

$$\epsilon_{yy}^o + e \frac{\partial^2 w}{\partial y^2} = \epsilon_r - e_r \frac{d^2 w_r}{dy^2} \quad (82)$$

$$w = w_r \quad (83)$$

2) Along  $y = b/2$

$$\epsilon_{xx}^o + e \frac{\partial^2 w}{\partial x^2} = \epsilon_s - e_s \frac{d^2 w_s}{dx^2} \quad (84)$$

$$w = w_s \quad (85)$$

Using Eqs. (26), (71), and (72) in conjunction with Eqs. (30-32), (77) and (79-81), Eqs. (82) and (83) lead to

$$q_n' = \sum_m (Z_{mn} q_m^s + \zeta_{mn} p_m^s) \quad (86)$$

$$p_n' = \sum_m (\bar{Z}_{mn} q_m^s + \bar{\zeta}_{mn} p_m^s) \quad (87)$$

Using Eqs. (8), (71), and (72) in conjunction with Eqs. (10), (11), (77), (79-81), Eqs. (84) and (85) lead to

$$W_{s0} = W_{00} + \sum_n (C_n q_n' + D_n p_n') \cos \frac{n\pi}{2} \quad (88)$$

$$\begin{aligned} \left( A_m + \sum_n \bar{A}_{mn} \cos \frac{n\pi}{2} \right) q_m^s + \left( B_m + \sum_n \bar{B}_{mn} \cos \frac{n\pi}{2} \right) p_m^s \\ + C_{m0} q_0' + \sum_n (\bar{C}_{mn} q_n' + \bar{D}_{mn} p_n') \cos \frac{n\pi}{2} \\ = A_m^s q_m^s + B_m^s p_m^s \end{aligned} \quad (89)$$

$$\begin{aligned} \left( A_m^u + \sum_n A_{mn}^u \cos \frac{n\pi}{2} \right) q_m^s + \left( B_m^u + \sum_n B_{mn}^u \cos \frac{n\pi}{2} \right) p_m^s \\ + C_{m0}^u q_0' + \sum_n (C_{mn}^u q_n' + D_{mn}^u p_n') \cos \frac{n\pi}{2} \\ = G_m^s p_m^s + (e + e_s) \alpha_m^2 (A_m^s q_m^s + B_m^s p_m^s) \end{aligned} \quad (90)$$

$$\epsilon_{s0} = X_{00} + \sum_n D_n^u p_n' \cos \frac{n\pi}{2} \quad (91)$$

and  $\epsilon_{r0}$  and  $W_{00}$  are related to  $q_0'$ ,  $q_m^s$ ,  $p_m^s$ , and  $W_{r0}$ .

Substituting Eqs. (86) and (87) into Eqs. (89) and (90), one obtains for each  $m$ ,

$$\begin{aligned} \left( A_m - A_m^s + \sum_n \bar{A}_{mn} \cos \frac{n\pi}{2} \right) q_m^s \\ + \left( B_m - B_m^s + \sum_n \bar{B}_{mn} \cos \frac{n\pi}{2} \right) p_m^s + C_{m0} q_0' \\ + \sum_n \bar{C}_{mn} \cos \frac{n\pi}{2} \sum_i (Z_{in} q_i^s + \zeta_{in} p_i^s) \\ + \sum_n \bar{D}_{mn} \cos \frac{n\pi}{2} \sum_i (\bar{Z}_{in} q_i^s + \bar{\zeta}_{in} p_i^s) = 0 \end{aligned} \quad (92)$$

$$\begin{aligned} \left[ A_m^u - (e + e_s) \alpha_m^2 A_m^s + \sum_n A_{mn}^u \cos \frac{n\pi}{2} \right] q_m^s \\ + \left[ B_m^u - (e + e_s) \alpha_m^2 B_m^s - G_m^s + \sum_n B_{mn}^u \cos \frac{n\pi}{2} \right] p_m^s \\ + C_{m0}^u q_0' + \sum_n C_{mn}^u \cos \frac{n\pi}{2} \sum_i (Z_{in} q_i^s + \zeta_{in} p_i^s) \\ + \sum_n D_{mn}^u \cos \frac{n\pi}{2} \sum_i (\bar{Z}_{in} q_i^s + \bar{\zeta}_{in} p_i^s) = 0 \end{aligned} \quad (93)$$

It is seen from Eqs. (92) and (93) that  $q_m^s$  and  $p_m^s$  can be determined if  $q_0'$  is represented in terms of  $q_m^s$ ,  $p_m^s$  and the

applied loading. The overall equilibrium of the skin and the stringer in the axial direction requires

$$\int_0^b N_x dy + P_s - \frac{1}{2} pab - \frac{b}{2\pi a} R = 0 \quad (94)$$

where  $R$  is the resultant force in the longitudinal direction without the effect of internal pressure.

Substituting Eqs. (2) and (47) into Eq. (94) using Eqs. (8), (11), (14), (73), and (78), and knowing that Eq. (94) must be satisfied for all values of  $x$ , one arrives at

$$b(A_{11}X_{00} + A_{12}Y_{00} - N_{xt}) + (EA)_s \epsilon_{s0} - P_{st} - \frac{1}{2} \left( pab + \frac{b}{\pi a} R \right) = 0 \quad (95)$$

Using Eqs. (81) and (91) in conjunction with Eq. (89), Eq. (95) becomes

$$\hat{B}_{11}X_{00} + \hat{B}_{12}q'_0 = \sum_m (\hat{A}_m q_m^s + \hat{B}_m p_m^s) + \sum_n \hat{D}_n p_n^r + \hat{T} + \frac{1}{2} \left( pab + \frac{b}{\pi a} R \right) \quad (96)$$

Using Eq. (81) in conjunction with Eq. (35) and  $W_{00}$ , Eq. (74) becomes

$$\hat{B}_{21}X_{00} + \hat{B}_{22}q'_0 = \sum_m (\bar{A}_m q_m^s + \bar{B}_m p_m^s) + paL + \bar{T} \quad (97)$$

Substituting Eq. (87) into Eq. (96) and solving the result with Eq. (97) simultaneously, one obtains

$$X_{00} = \sum_m (a_{xm} q_m^s + b_{xm} p_m^s) + D \left[ \hat{B}_{22} \hat{T} - \hat{B}_{12} \bar{T} + \left( \hat{B}_{22} \frac{b}{2} - \hat{B}_{12} L \right) pa + \frac{b}{2\pi a} \hat{B}_{22} R \right] \quad (98)$$

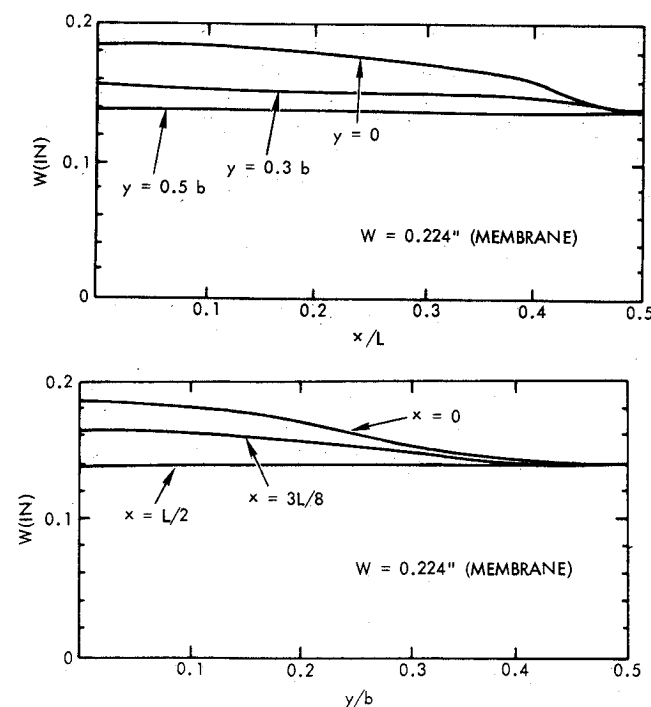


Fig. 5 Normal displacement ( $p = 10$  psi).

$$q'_0 = \sum_m (a_m q_m^s + b_m p_m^s) + D \left[ \hat{B}_{11} \bar{T} - \hat{B}_{21} \hat{T} + \left( \hat{B}_{11} L - \hat{B}_{21} \frac{b}{2} \right) pa - \frac{b}{2\pi a} \hat{B}_{21} R \right] \quad (99)$$

where all coefficients are known constants.

Substituting Eq. (99) into Eqs. (92) and (93), one obtains the following infinite set of algebraic equations:

$$\begin{bmatrix} G_{mj} & J_{mj} \\ L_{mj} & H_{mj} \end{bmatrix} \begin{Bmatrix} q_j^s \\ p_j^s \end{Bmatrix} = \begin{Bmatrix} C_{m0} \\ C_{u0} \end{Bmatrix} D \left( Bp + H_t + \frac{b}{2\pi a} \hat{B}_{21} R \right) \quad (100)$$

where all coefficients can be expressed in terms of known constants.

Upon truncation of various series to a finite number of terms,  $q_i^s$  and  $p_i^s$  can be obtained from Eq. (100). Once  $q_i^s$  and  $p_i^s$  are calculated, all other quantities can subsequently be computed.

### Numerical Example

For illustrative purposes, an example with the following data is considered:

$$L = 20 \text{ in.}, \quad a = 117.5 \text{ in.}, \quad b = 5.8 \text{ in.}, \quad h = 0.075 \text{ in.}$$

$$(EI)_r = 0.269 \times 10^8 \text{ lb} \cdot \text{in.}^2,$$

$$(EA)_r = 0.592 \times 10^7 \text{ lb}, \quad e_r = 3.78 \text{ in.}$$

$$(EI)_s = 0.142 \times 10^8 \text{ lb} \cdot \text{in.}^2,$$

$$(EA)_s = 0.404 \times 10^7 \text{ lb}, \quad e_s = 1.10 \text{ in.}$$

$$R_0 = 113.72 \text{ in.}, \quad c_s/2 = 0.53 \text{ in.}, \quad c_r/2 = 0.375 \text{ in.}$$

$$[A_{ij}] = \begin{bmatrix} 0.664 & 0.221 & 0 \\ 0.221 & 0.577 & 0 \\ 0 & 0 & 0.221 \end{bmatrix} \times 10^6 \text{ lb/in.}$$

$$[D_{ij}] = \begin{bmatrix} 262 & 159 & 4.33 \\ 159 & 210 & 4.33 \\ 4.33 & 4.33 & 159 \end{bmatrix} \text{ in./lb}$$

The membrane solutions corresponding to internal pressure  $p$  without the effect of stiffeners are

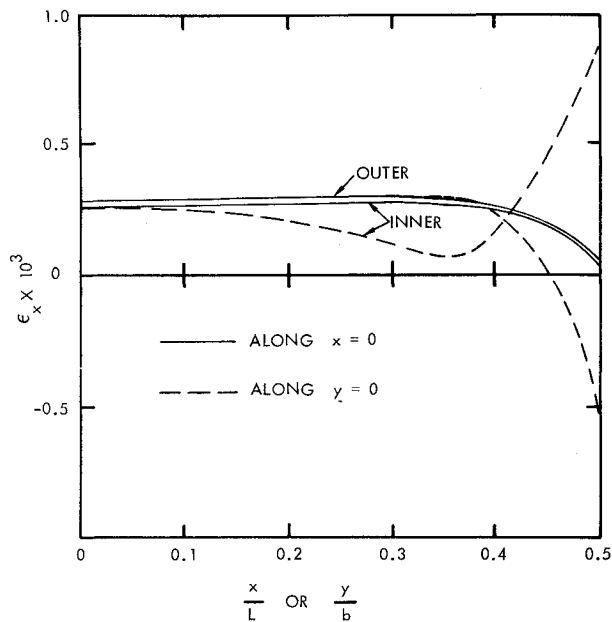
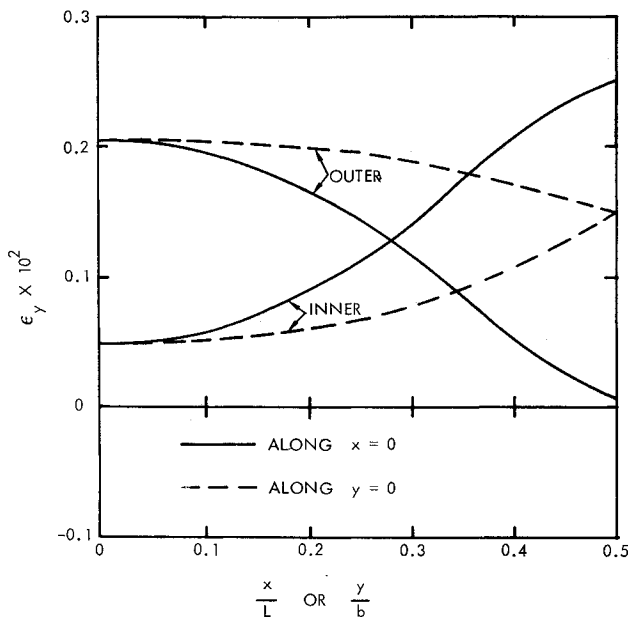
$$N_x = \frac{1}{2} pa = 58.75p \quad N_y = pa = 117.5p$$

$$w = pa^2 (\frac{1}{2} B_{21} + B_{22}) = p (117.5)^2 [ - (0.66/2) + 1.95 ] \times 10^{-6} = 0.022366p$$

Results correspond to various effects including internal pressure  $p$ , temperature change  $T$ , externally applied longitudinal resultant force  $R$  are examined individually. All results are computed based on the maximum value of  $m$  and  $n$  of 20.

### Case 1

Various results corresponding to internal pressure  $p = 10$  psi are presented in Figs. 5-7. Figure 5 shows the variation of normal displacement at various locations of the skin. Curves shown in Fig. 5 indicate the bulging or pillowing of the skin due to stiffeners. The maximum displacement occurring at  $x = y = 0$  as expected is slightly under 82% of the membrane solution of 0.224 in. The minimum displacement occurring at the ring location amounts to 62% of the membrane solution.

Fig. 6 Longitudinal strain ( $p = 10$  psi).Fig. 7 Circumferential strain ( $p = 10$  psi).

The longitudinal stress resultant  $N_x$  of 435-440 lb/in. has minor variations. As the resultant force of  $N_x$  in the skin at its lowest value is equal to  $435 \times 5.8 = 2523$  lb., the longitudinal force carried by each stringer at its highest value becomes  $[(0.5)(10)(117.5)(5.8) - 2523] = 884.5$  lb. It may be noted that, although the extensional stiffness of the stringer ( $4.04 \times 10^6$  lb) is comparable but higher than the total longitudinal stiffness of the skin ( $0.664 \times 10^6 \times 5.8 = 3.85 \times 10^6$  lb), the skin carries a substantially larger percentage of total longitudinal force of  $(0.5)(10)(117.5)(5.8) = 3407.5$  lb due to the closed-end effect.

The circumferential stress resultant  $N_y$  ranges 784-888 lb/in. and has noticeable variation along the longitudinal coordinates. However, there is negligible variation with respect to the circumferential coordinate. The value of  $N_y$  increases from the midsection between the rings toward the ring location. This trend may be attributed to the shear lag effect.

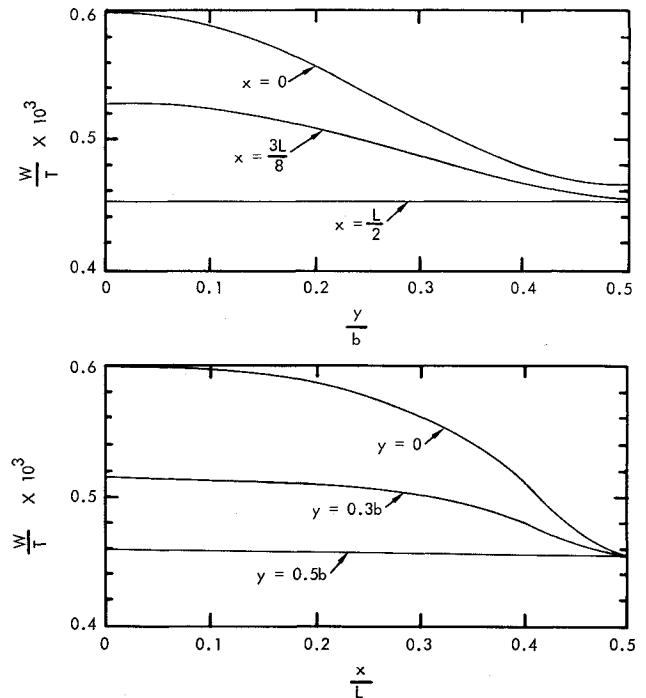


Fig. 8 Normal displacement.

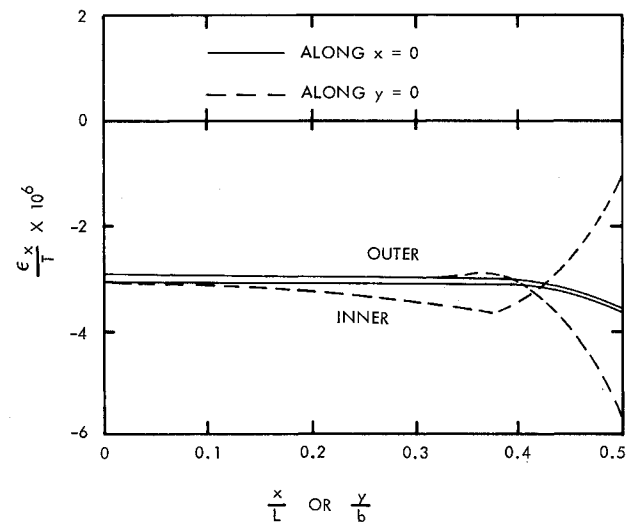


Fig. 9 Longitudinal strain.

The bulging or pillowing effect results in the bending of the skin. The extensional strains at the inner and outer surfaces of the skin at various locations are plotted in Figs. 6 and 7. The severe locations due to the pillowing effect occurs at the stiffeners.

#### Case 2

Various results corresponding to constant temperature change  $T$  are presented in Figs. 8-10. The coefficients of thermal expansion in the longitudinal and circumferential directions are taken to be  $\alpha_1 = 6.4 \times 10^{-6}$  in./in./°F and  $\alpha_2 = 5.2 \times 10^{-6}$  in./in./°F, respectively. Consequently,

$$N_{xt} = (\alpha_1 B_{11} + \alpha_2 B_{12})T = 5.4T$$

$$N_{yt} = (\alpha_1 B_{21} + \alpha_2 B_{22})T = 4.4T$$

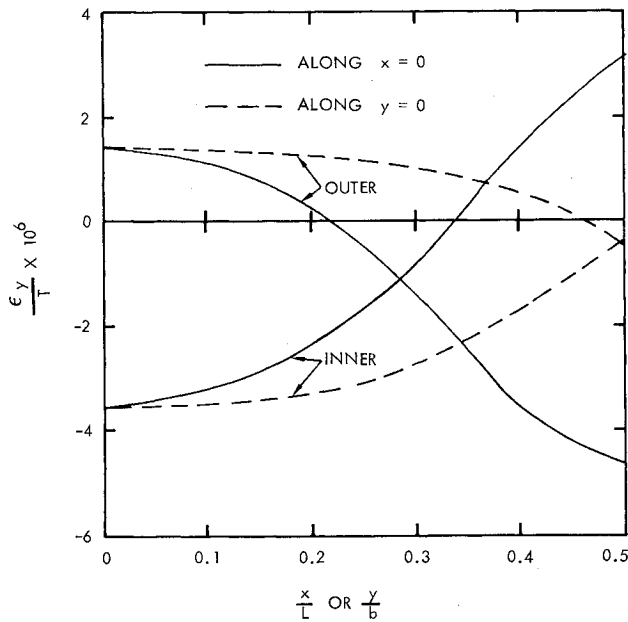


Fig. 10 Circumferential strain.

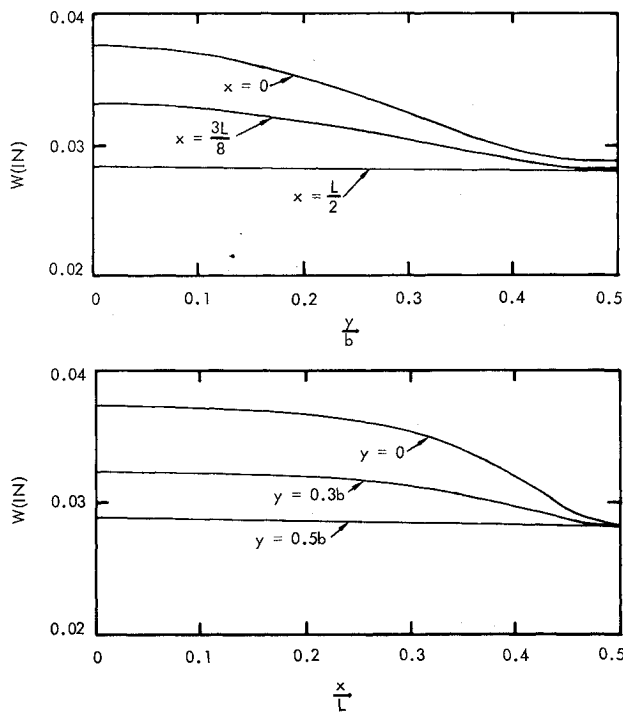


Fig. 11 Normal displacement ( $R = -10^6$  lb).

are considered. The temperature change occurring in the skin only is assumed in the example. The coefficients  $B_{ij}$  are the elements of the inverse of the  $[A_{ij}]$  matrix.

### Case 3

Various results corresponding to longitudinal resultant force  $R = -10^6$  lb are presented in Figs. 11-13. The variation of longitudinal stress resultant  $N_x$  is small. The maximum and minimum computed compressive values are 652 and 602 lb/in., respectively. If one smears the longitudinal extensional stiffness of the skin and stringers, the average longitudinal stress resultant in the skin would be

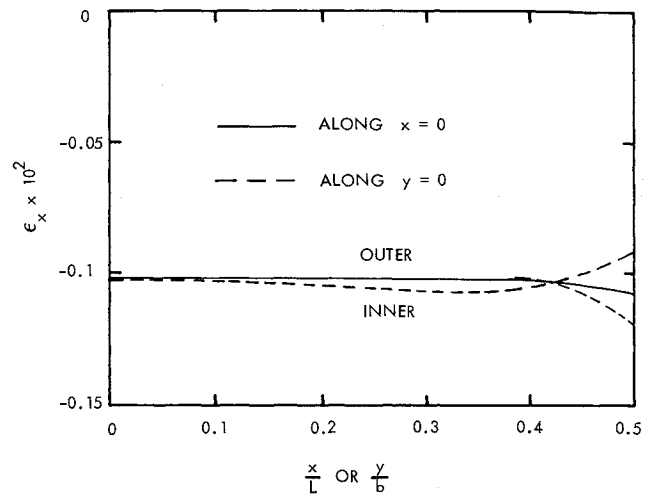


Fig. 12 Longitudinal strain ( $R = -10^6$  lb).

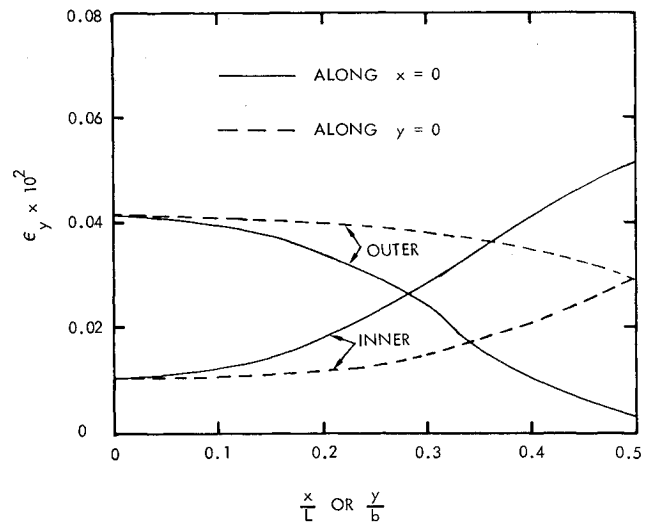


Fig. 13 Circumferential strain ( $R = -10^6$  lb).

$$\frac{R}{2\pi a} \cdot \frac{D_{11}}{D_{11} + [(EA)_r/b]} = \frac{-10^6}{2\pi(117.5)} \cdot \frac{0.664}{0.664 + 4.04/5.8} = -693.5 \text{ lb/in.}$$

which means that the stringers have carried a greater share of the load from the relative stiffness standpoint.

### Conclusions

Orthotropic cylindrical shells stiffened orthogonally by equally spaced rings and stringers subjected to uniform pressure, temperature change, and axial load have been analyzed by treating the shell, stringers, and rings as discrete components. The analysis allows one to calculate the stresses, strains, and displacements at any point in the stiffened shell. The closed-end effect is included in the analysis, which represents an improvement of the previous analysis on orthogonally stiffened isotropic shells.<sup>1</sup>

### Acknowledgments

Valuable discussions, suggestions and advice generously provided by S. B. Biggers, L. W. Liu, and J. N. Dickson of



Lockheed-Georgia Company during the investigation are gratefully acknowledged.

### References

<sup>1</sup>Wang, J.T.S., "Orthogonally Stiffened Cylindrical Shells Subjected to Internal Pressure," *AIAA Journal*, Vol. 6, 1970, pp. 455-461.

<sup>2</sup>Stephens, W. B., "Imperfection Sensitivity of Axially Compressed Stringer Reinforced Cylindrical Panels under Pressure," *AIAA Journal*, Vol. 9, 1971, pp. 1713-1719.

<sup>3</sup>Tvergaard, V., "Buckling of Elastic-Plastic Cylindrical Panel under Axial Compression," *International Journal of Solids and Structures*, Vol. 13, 1977, pp. 957-970.

<sup>4</sup>Rinehart, S. A. and Wang, J.T.S., "Vibration of Simply Supported Cylindrical Shells with Longitudinal Stiffeners," *Journal of Sound and Vibration*, Vol. 24, 1972, pp. 151-163.

<sup>5</sup>Wang, J.T.S. and Lin, Y. J., "Stability of Discretely Stringer-Stiffened Cylindrical Shells," *AIAA Journal*, Vol. 11, 1973, pp. 810-814.

<sup>6</sup>Wang, J.T.S. and Rinehart, S. A., "Free Vibrations of Longitudinally Stiffened Cylindrical Shells," *Journal of Applied Mechanics, Transactions of ASME*, Vol. 41, 1974, pp. 1087-1093.

<sup>7</sup>Reddy, B. D., "Buckling of Elastic-Plastic Discretely Stiffened Cylinders in Axial Compression," *International Journal of Solids and Structures*, Vol. 16, 1980, pp. 313-328.

*From the AIAA Progress in Astronautics and Aeronautics Series . . .*

## GASDYNAMICS OF DETONATIONS AND EXPLOSIONS—v. 75 and COMBUSTION IN REACTIVE SYSTEMS—v. 76

*Edited by J. Ray Bowen, University of Wisconsin,  
N. Manson, Université de Poitiers,  
A. K. Oppenheim, University of California,  
and R. I. Soloukhin, BSSR Academy of Sciences*

The papers in Volumes 75 and 76 of this Series comprise, on a selective basis, the revised and edited manuscripts of the presentations made at the 7th International Colloquium on Gasdynamics of Explosions and Reactive Systems, held in Göttingen, Germany, in August 1979. In the general field of combustion and flames, the phenomena of explosions and detonations involve some of the most complex processes ever to challenge the combustion scientist or gasdynamicist, simply for the reason that *both* gasdynamics and chemical reaction kinetics occur in an interactive manner in a very short time.

It has been only in the past two decades or so that research in the field of explosion phenomena has made substantial progress, largely due to advances in fast-response solid-state instrumentation for diagnostic experimentation and high-capacity electronic digital computers for carrying out complex theoretical studies. As the pace of such explosion research quickened, it became evident to research scientists on a broad international scale that it would be desirable to hold a regular series of international conferences devoted specifically to this aspect of combustion science (which might equally be called a special aspect of fluid-mechanical science). As the series continued to develop over the years, the topics included such special phenomena as liquid- and solid-phase explosions, initiation and ignition, nonequilibrium processes, turbulence effects, propagation of explosive waves, the detailed gasdynamic structure of detonation waves, and so on. These topics, as well as others, are included in the present two volumes. Volume 75, *Gasdynamics of Detonations and Explosions*, covers wall and confinement effects, liquid- and solid-phase phenomena, and cellular structure of detonations; Volume 76, *Combustion in Reactive Systems*, covers nonequilibrium processes, ignition, turbulence, propagation phenomena, and detailed kinetic modeling. The two volumes are recommended to the attention not only of combustion scientists in general but also to those concerned with the evolving interdisciplinary field of reactive gasdynamics.

*Published in 1981, Volume 75—446 pp., 6×9, illus., \$35.00 Mem., \$55.00 List  
Volume 76—656 pp., 6×9, illus., \$35.00 Mem., \$55.00 List*

TO ORDER WRITE: Publications Dept., AIAA, 1633 Broadway, New York, N.Y. 10019